Air Quality, Atmosphere & Health (2023) 16:641–659
https://doi.org/10.1007/s11869-022-01294-w

Impact of the COVID-19 pandemic on air pollution from jet engines at airports in central eastern China

Danwen Bao[1] · Shijia Tian[1] · Di Kang[2] · Ziqian Zhang[1] · Ting Zhu[1]

Received: 14 June 2022 / Accepted: 25 November 2022 / Published online: 5 December 2022

Abstract

Aircraft engine emissions (AEEs) generated during landing and takeoff (LTO) cycles are important air pollutant sources that directly impact the air quality at airports. Although the COVID-19 pandemic triggered an unprecedented collapse in the civil aviation industry, it also relieved some environmental pressure on airports. To quantify the impact of COVID-19 on AEEs, the amounts of three typical air pollutants (i.e., HC, CO, and NO_x) from LTO cycles at airports in central eastern China were estimated before and after the pandemic. The study also explored the temporal variation and the spatial autocorrelation of both the emission quantity and the emission intensity, as well as their spatial associations with other socioeconomic factors. The results illustrated that the spatiotemporal distribution pattern of AEEs was significantly influenced by the policies implemented and the severity of COVID-19. The variations of AEEs at airports with similar characteristics and functional positions generally followed similar patterns. The results also showed that the studied air pollutants present positive spatial autocorrelation, and a positive spatial dependence was found between the AEEs and other external socioeconomic factors. Based on the findings, some possible policy directions for building a more sustainable and environment-friendly airport group in the post-pandemic era were proposed. This study provides practical guidance on continuous monitoring of the AEEs from LTO cycles and studying the impact of COVID-19 on the airport environment for other regions or countries.

Keywords Aircraft engine emission · Coronavirus pandemic · Hydrocarbons · Carbon monoxide · Nitrogen oxides · Spatial dependence

Introduction

The civil aviation industry has witnessed decades of steady growth until the outbreak of the novel coronavirus disease 2019 (COVID-19). While air travel has made it possible for passengers to reach more remote destinations in less time and at affordable costs, it has also contributed to the global spread of infectious diseases (Sun et al. 2020; Linka et al. 2021). To slow down the transmission of COVID-19, up to 194 countries have implemented measures to restrict individuals' mobility in response to the pandemic (Lee et al. 2020). The heavy travel restrictions, together with the unprecedented decrease in passenger demand, have adversely impacted the civil aviation industry (Dube et al. 2021). Airlines have placed numerous aircraft types into temporary storage to avoid significant financial loss from flying empty planes (Adrienne et al. 2020). And many airports had to close their runways to make room for aircraft parking or just significantly limited their operations, awaiting traffic to pick up again. Consequently, there was a substantial decline in domestic and international passenger flights worldwide (Sun et al. 2021). According to International Civil Aviation Organization (ICAO 2020), the overall number of passengers by April had fallen 92% from 2019 levels, an average of a 98% drop-off in international traffic and 87% in domestic air travel. Evidence showed that the decline in air passenger traffic caused by COVID-19 was far more significant than that caused by other effects in literature (Xue et al. 2021b). Although flight suspensions negatively affect many aspects of society, it is expected to have some positive effects on the environment.

✉ Shijia Tian
Lexi_tian@126.com

[1] College of Civil Aviation, Nanjing University of Aeronautics and Astronautics, Jiangning District, No. 29, Jiangjun Avenue, Nanjing 211106, Jiangsu Province, China

[2] Department of Industrial and Systems Engineering, University of Minnesota, 2818 Como Avenue S.E, Minneapolis, MN 55414, USA

One of the most prominent influences that aviation has on the environment is air pollution (Brasseur et al. 2016). Aircraft engines exhaust gases and particles, including carbon monoxide (CO), nitrogen oxides (NO_x), sulfur oxide (SO_x), hydrocarbons (HC), particulate matter (PM), and so forth (Kurniawan and Khardi 2011). Conventionally, the operations of aircraft are divided into two phases: The landing and takeoff (LTO) phase, which occurs at an altitude below 3000 ft, and the cruise phase, which takes place at an altitude above 3000 ft (Kurniawan and Khardi 2011). Aircraft engine emissions (AEEs) at the cruising altitude are directly released into the upper troposphere and the lower stratosphere, which mainly impact climate change (Brasseur et al. 2016), while AEEs from LTO cycles are primarily associated with the deterioration of air quality at the ground level (Amato et al. 2010; Hsu et al. 2012). Although aircraft emits gases and particles primarily during the cruise phase, AEEs from LTO cycles have aroused increasing public concern in recent years due to the following reasons: (i) In the year 2019, researchers from the Massachusetts Institute of Technology have uncovered that aviation causes twice as much damage to air quality as it does to the climate (Lang 2019); (ii) AEEs from LTO cycles have a more direct effect on human health, local eco-system, and cultural heritage, which are closely related to the living standards of human beings (Song et al. 2019; Aygun and Caliskan 2021; Głowacki et al. 2022). Therefore, the estimation of AEEs from LTO cycles has been recognized as an important issue for developing strategies as future guidelines for airport environmental sustainability.

It is widely acknowledged that 2020 is an unusual year for the civil aviation industry as the COVID-19 outbreak is the first major global pandemic in the era of passenger jet air transportation since the late 1950s (Elias 2020). Accordingly, this study intends to explore the positive environmental impacts of travel restrictions from the perspective of AEEs at the ground level. Although several researches have focused on the estimation and analysis of AEEs from LTO cycles at both the local scale (Yılmaz 2017; Kuzu 2018; Tokuslu 2020) and the regional scale (Kesgin 2006; Hu et al. 2020; Yu et al. 2021), the research on AEEs from LTO cycles in the context of the COVID-19 pandemic is still scarce. Furthermore, there has never been any analysis of the relative change in air pollution at airports between the COVID-19 era and the pre-COVID-19 era, either from a temporal or spatial perspective. In addition, the spatial spillover effect of AEEs and the spatial association with local socioeconomic factors have not been studied yet. Therefore, we explore this area to better comprehend the disparities in the variation patterns of AEEs and its correlations with both COVID-19-related factors and socioeconomic factors.

This paper aims to answer the following research questions: (i) How do the relative changes of the studied AEEs distributed temporally and geographically? And how do the spread of COVID-19 and pertinent policy responses impact the variation patterns? (ii) Does the variation of AEEs at airports with similar characteristics and functional positions follow a specific pattern? (iii) Are AEEs at airports in the studied region spatially dependent? (iv) Does spatial association exist between the socioeconomic status of cities nearby and the AEEs at local airports? To answer these questions, we first analyzed the distribution patterns of relative change on both geographical and temporal scales. Using a modified k-means clustering algorithm, the studied airports were then categorized into groups based on their AEE variation characteristics. Furthermore, some spatial statistical indicators, including univariate and bivariate Moran's Index (i.e., Moran's I), were calculated to assess the existence of spatial autocorrelation and spatial association. Based on the results and discussions, the corresponding policy implications were provided.

The remainder of this study is organized as follows. In the second section, relevant literature is briefly reviewed. The third section presents the geographical scope, data sources, variables, and methods. The results are presented and discussed in the fourth section. The fifth section suggests the policy implications. The last section provides the main conclusions and recommendations for future research.

Literature review

A number of studies have investigated the impacts of COVID-19 on transport-related air pollution. Table 1 summarizes the main findings in existing studies on the effects of COVID-19 on traffic-caused air pollution. Compared to road and marine traffic, air pollution caused by air traffic received comparatively less attention. The majority of the studies, which measured the AEEs at airports, were conducted before the outbreak of COVID-19. Yılmaz (2017) estimated the HC, CO, and NO_x from the LTO cycle at Kayseri Airport, Turkey. Similar research was also conducted at Los Angeles International Airport (Shirmohammadi et al. 2017), Detroit Metropolitan Airport (Ashok et al. 2017), Atatürk International Airport (Kuzu 2018), and Georgian International Airport (Tokuslu 2021). However, these studies mainly focused on investigating the distribution of total LTO emissions for each operation mode at a single airport. As for the regional multi-airport scale, Song and Shon (2012) calculated the emissions of greenhouse gases at four major international airports in Korea. It was found that monthly and daily emissions do not vary significantly. Yu et al.

Table 1 Literature on the effects of COVID-19 on traffic-caused air pollution

Study	Type of traffic	Major finding
Xiang et al. (2020)	Road	Due to the stay home order (SHO) restriction, the median PM2.5, NO_x, and CO levels near the freeway in downtown Seattle significantly declined by 33%, 30%, and 17%, respectively
Wu et al. (2021)	Road	CO declined by 28.8% at roadside stations in Shanghai due to the COVID-19 lockdown. The decrease in NO_x from vehicles led to an increase in ozone on the roadside (30.2%)
Collivignarelli et al. (2020)	Road	The restriction of mobility led to a significant decrease in the concentration of air pollutants mainly due to vehicular traffic (PM2.5, PM10, BC, benzene, CO, and NOx)
Nakada and Urban (2020)	Road	During the partial lockdown in São Paulo, Brazil, an increase of approximately 30% in ozone concentration was observed, probably related to NO_x decreases influenced by vehicle traffic
Shi and Weng (2021)	Water	As a result of the strict COVID-19 quarantine measures, the emissions from cargo ship are significantly reduced, while the emissions from the container ships and tankers slightly decreased
Ju and Hargreaves (2021)	Water	A significant decrease in CO_2 occurred from June to August 2020 in Singapore as most of the marine transport of essential goods remained normal despite the COVID-19 epidemic
Xue et al. (2021a, b)	Air	Since the second quarter of 2020, daily fuel consumption and aircraft emissions have been rising in four Chinese international airports. In the fourth quarter, the ratio of 2020 to 2019 is 0.875
Cui et al. (2022)	Air	Affected by the epidemic, the average emissions from the climbing, cruising, and descending stages of the routes decreased significantly in South America

(2021) analyzed the trend of AEEs at some airports in mainland China from 1970 to 2017 and found that the average emission per passenger has declined for the duration. Bao et al. (2021) revealed some simple regional distribution of AEEs from LTO cycles during the pandemic but failed to thoroughly compare the AEEs at airports in 2020 to the year when the pandemic had not yet occurred. Although these studies have provided valuable insights for investigating the ground-level AEEs from a regional cooperative perspective, they rarely consider the spatial interaction and spatial spillover effects within the region and how their effects on the distribution of emission quantity (EQ) and emission intensity (EI, i.e., emission per passenger). In addition, to the authors' knowledge, the spatial correlation between AEEs from LTO cycles and other socioeconomic factors has not been examined using spatial econometric methods in any literature.

Overall, research on AEEs from LTO cycles in the context of the COVID-19 pandemic is still limited. Although several attempts have brought valuable results of emissions from the aircraft engines during each operation mode of a typical LTO, the impact of COVID-19 on the spatiotemporal distribution of EQ, EI, and their relative change still needs further research. The LTO emission data at an individual airport has rarely been viewed as geo-referenced data, which considers the impact of the adjacent areas. Given this, we found it necessary to fill the aforementioned research gaps. With the employment of some other analytical methodologies, the following contributions have been made in this research compared to the previous studies: (i) To better comprehend the COVID-19 impact on airport environment, special attention was devoted to both EQ and EI, as well as their relative changes between the pre-COVID-19 era and the year 2020. (ii) The temporal variation patterns of AEEs during the COVID-19 pandemic were classified, and the potential causes were analyzed. (iii) The spatial dependence effect of both the EQ and EI, and their association with other socioeconomic factors were investigated in this paper.

Materials and methods

Geographical scope

The Yangtze River Delta (YRD), which consists of Jiangsu province, Zhejiang province, Anhui province, and Shanghai municipality, is a major metropolitan area located in the east of China (Fig. 1). Accounting for about 23% of the total gross domestic product (GDP) and 11% of the total population, the YRD is widely recognized as a significant driving force for the nation's economy. In December 2019, the government issued an outline for the integrated development of the YRD. Tasks specified in the outline include establishing a world-class regional airfield complex. Table 2 shows the basic information of the airports at the YRD. Currently, there are 22 civil airports in the YRD, including 2 airports in Shanghai, 9 airports in Jiangsu, 6 airports in Zhejiang, and 5 airports in Anhui province. And the 4 largest airports, which served more than 100,000 flights in 2020, are the airports in Shanghai, Hangzhou, and Nanjing. The outline pointed out that it is crucial to ensure that the airports are under coordinated management within the region. Despite the region's outstanding performance in civil aviation, the extensive air pollution related to air traffic is still a challenging problem due to the high volume of flights.

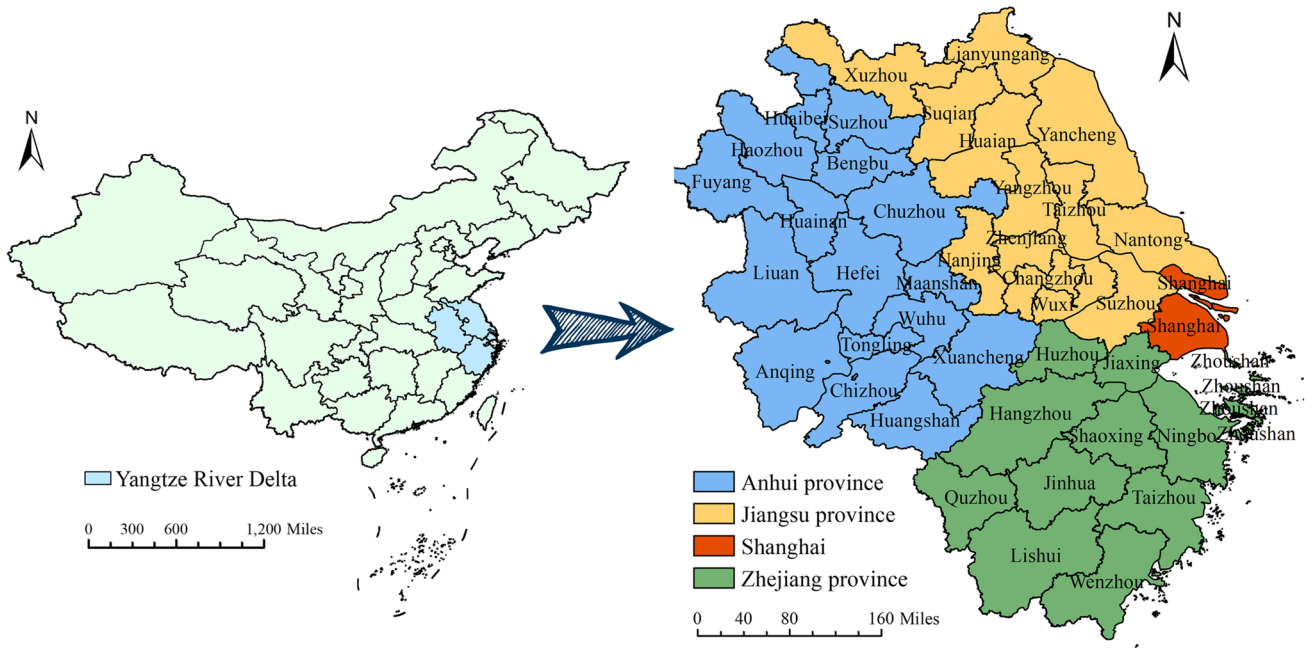

Fig. 1 The map of the Yangtze River Delta, China

Table 2 The basic information of airports in the Yangtze River Delta

Province	Airport name	IATA codes	City	Flight demand of 2020
Shanghai	Shanghai Pudong International Airport	PVG	Shanghai	325,678
	Shanghai Hongqiao International Airport	SHA	Shanghai	219,404
Jiangsu	Changzhou Bennou International Airport	CZX	Changzhou	22,000
	Huaian Lianshui International Airport	HIA	Huaian	34,135
	Lianyungang Baita International Airport	LYG	Lianyungang	11,826
	Nantong Xingdong International Airport	NTG	Nantong	28,454
	Sunnan Shuofang International Airport	WUX	Wuxi	53,901
	Xuzhou Guanyin International Airport	XUZ	Xuzhou	34,568
	Yancheng Nanyang International Airport	YNZ	Yancheng	18,799
	Yangzhou Taizhou International Airport	YTY	Yangzhou	42,154
	Nanjing Lukou International Airport	NKG	Nanjing	181,724
Zhejiang	Ningbo Lishe International Airport	NGB	Ningbo	75,373
	Taizhou Luqiao Airport	HYN	Taizhou	9492
	Wenzhou Yongqiang International Airport	WNZ	Wenzhou	73,717
	Yiwu Airport	YIW	Jinhua	13,677
	Zhoushan Putuoshan Airport	HSN	Zhoushan	20,250
	Hangzhou Xiaoshan International Airport	HGH	Hangzhou	237,362
Anhui	Anqing Tianzhushan Airport	AQG	Anqing	5328
	Chizhou Jiuhuashan Airport	JUH	Chizhou	3034
	Fuyang Xiguan Airport	FUG	Fuyang	13,712
	Huangshan Tunxi International Airport	TXN	Huangshan	5526
	Hefei Xinqiao International Airport	HFE	Hefei	74,391

The outline also stressed that priority should be given to environmental protection. Therefore, to better understand aviation-related environmental issues, it is necessary to study the spatiotemporal pattern of the AEEs generated during LTO cycles at the airports in the YRD.

Data resources

Different types of data are needed for estimating the amount of AEEs released during LTO cycles. Firstly, the information on daily flights at 22 airports in the YRD from January 1, 2019 to December 31, 2020 was obtained from the Official Airline Guide (OAG) company (www.oag.com), the world's leading travel data provider. With the world's largest network of flight information data, OAG provides access to the most accurate airline schedules and flight records. The historical flight status database includes records of flight information, which contains the flight number, the operating time, the carrier, the origin airport, the departure airport, the aircraft name, which can be specific to a certain series of an aircraft type, etc. The number of daily LTO cycles and the accurate aircraft type of each flight were collected from those records. The aircraft-engine combination was determined by the information from the official websites of aircraft manufacturers and airlines. In an entire LTO cycle, the power setting (%), the time spent (minutes), fuel flow (kg/s), and the emission indices of the HC, NO_x, and CO of a certain engine type for each operation mode (i.e., idle, approach, climb out, and takeoff) were obtained from the ICAO engine emission databank.

Methodology

Aircraft emission calculation model

HC, CO, and NO_x are the reference AEEs defined in ICAO standards against which engines are certificated (Nielsen et al. 2019). To best reflect actual emission quantity of HC, CO, and NO_x, we employed an advanced approach recommended by ICAO (2016). The equation below shows the formula to calculate the AEEs during LTO cycles.

$$EQ_i = \sum_j \sum_{m=1}^{4} LTO_j \times NE_j \times FC_{j,m} \times \left(\frac{TIM_{j,m}}{60}\right) \times EI_{i,j,m} \quad (1)$$

Where i is the type of AEEs (i.e., HC, CO, and NO_x); j is the type of aircraft; m is the operation mode in a typical LTO cycle (i.e., idle, approach, takeoff, and climb out); EQ_i is the total emission of pollutant i , in grams (g); LTO_J is the number of the LTO cycle for aircraft j; NE_j is the number of engine of aircraft j;$FC_{j,m}$ is the fuel consumption of aircraft j in mode m , in kilograms per second (kg/s); $TIM_{j,m}$ is the duration (abbreviation of time in mode) of mode m for aircraft j, in minutes (min); $EI_{i,j,m}$ is the emission factor for pollutant i, aircraft j in operating mode m, in grams per pollutant per kilogram of fuel (g/kg of fuel) for each engine on aircraft j.

Clustering algorithm

Clustering analysis can search for correlations among time series data (Wu et al. 2022). To classify the temporal variation pattern of the AEEs, a modified k-means clustering algorithm is used to partition the variations of AEEs at different airports into homogeneous subgroups. Firstly, the percentage of the change in the emissions between every two consecutive months in 2020 was calculated. Then, to best feature the variation of the emission between each consecutive 2 months, we further classify the change of AEEs into five categories: (i) substantial decrease, i.e., a decline that is smaller than − 50%; (ii) moderate decrease, i.e., a decline from − 50 to − 10%; (iii) stability, i.e., a decline from − 10 to 0% and a growth from 0 to 10%; (iv) moderate increase, i.e., a growth from 10 to 50%; (v) substantial increase, i.e., a growth that is larger than 50%. The five variation categories are labeled − 2, − 1, 0, 1, and 2, respectively. Since there are 11 intervals between 12 months, each airport in the YRD can be labeled by 11 numbers based on the variation trend of the AEEs. The series of numbers of different airports are then selected to be the input dataset for the clustering algorithm. And the airports can, therefore, be categorized into clusters using the K-means clustering method. Airports that belong to the same cluster have similar variation trends.

Spatial dependence analysis

Spatial dependence is an essential property within the geographic space: characteristics at adjacent locations tend to be positively or negatively correlated. Such a phenomenon results from several spatial effects, including spatial interaction, spatial hierarchies, and spatial spillover (Cartone et al. 2021).

A spatial weight matrix quantifies the spatial relationships between the observational units in a spatially referenced dataset (Fotheringham and Brunsdon 1999). It is an $n \times n$ positive symmetric matrix, denoted as W, with element w_{ij} at location i, j for n locations. According to the spatial data type, the spatial weights can be classified into two categories: contiguity-based weights and distance-based weight. Contiguity-based weights are commonly adopted to measure the adjacency of polygons, and contiguity means that two spatial units share a common border of non-zero length. In comparison, distance-based weights are usually adopted for measuring the relative locations between points (Negret et al. 2020). Since the observations of the study are

not based on cities (whose shapes are polygons) within the research region but on the airports (which can be seen as separate points) within each city, the distance-based spatial weight matrix is more suitable to represent the spatial structure of the research data. The most widely used distance-based weighting method is inverse distance squared weighting, which is in accordance with the logic of Tobler's geography law (Musashi et al. 2018). Taking the theory of impedance and distance decay into consideration (Simini et al. 2012), the inverse distance squared weighting assumes that each measured point has a local influence on the others that diminishes with distance, and the superiority of it in modeling autocorrelation function has been demonstrated in several literatures (Ping et al. 2004; Musashi et al. 2018). Therefore, the element in the weight matrix is calculated by the following formula:

$$w_{ij} = \frac{1}{d_{ij}^2} \tag{2}$$

Where d_U is the distance from the center of unit i to the neighboring unit j

To investigate whether the AEEs from LTO cycles at the studied airports in the YRD are spatially correlated, a spatial autocorrelation analysis is conducted by calculating both the global and the local Moran's I developed by Moran (1950) and Anselin (1995). The value of Moran's I ranges from − 1 to 1. A positive Moran's I indicates the clustering of similar values, while a negative Moran's I indicates the clustering of dissimilar values (i.e., dispersion). A value of 0 for Moran's I typically indicates no autocorrelation, which means that the values are randomly distributed. The larger the absolute value of Moran's I is, the stronger the spatial autocorrelation exists. The global Moran's I assesses the overall spatial autocorrelation in the research region, as shown in Eq. (3). The local Moran's I is the statistic for local indicators of spatial association (LISA), which is a localized measure of the spatial aggregation of AEEs around airport i, as shown in Eq. (4).

$$I_U = \left(\frac{n}{\sum_{i=1}^{n}\sum_{j=1}^{n} w_{ij}}\right)\left(\frac{\sum_{i=1}^{n}\sum_{j=1}^{n} w_{ij}\left(x_i-\bar{x}\right)\left(y_i-\bar{y}\right)}{\sum_{i=1}^{n}\left(x_i-\bar{x}\right)^2}\right) \tag{3}$$

$$I_{Ui} = \frac{n\left(x_i-\bar{x}\right)}{\sum_{i=1}^{n}\left(x_i-\bar{x}\right)^2}\sum_{j=1}^{n} w_{ij}\left(w_j-\bar{x}\right) \tag{4}$$

where I_U refers to the global univariate Moran's I; I_{Ui} represents the local univariate Moran's I for airport i; • w_{ij} is the element of the spatial weight matrix; x_i and x_j are the amounts of AEEs at airport i and airport j, respectively; $\bar{x}$ is the average amount of AEEs; n is the number of airports in the YRD.

To explore how AEEs at airports spatially correlate with other socioeconomic factors in the adjacent areas within the research region, a cross-correlation analysis is conducted by calculating the bivariate Moran's I. Common bivariate association measures, such as Person's correlation coefficient, fail to recognize the spatial interaction of the dataset. Tobler (1979) summarizes the first theory of geography as, "Everything is related to everything else, but near things are more related than distant things." According to this theory, no region is isolated, and each region is continuously developing in accordance with its correlation with other regions (Ma et al. 2015). Therefore, by adopting both the concept of the Person's correlation and univariate Moran's I, bivariate Moran's I was developed to capture bivariate spatial dependence (Lee 2001). In this study, the global bivariate Moran's I measures the overall spatial dependence between AEEs and other socioeconomic factors, as defined in Eq. (5). In contrast, the bivariate LISA can reveal the spatial disparity of the association at the local level, as defined in Eq. (6). The pseudo-significance of the bivariate Moran' I statistics is evaluated at the 5% level based on 10,000 randomization permutations, which can reduce the uncertainty to an acceptable level. The bivariate Moran's I with p-values below 5% indicates that the amount of AEEs at a particular airport is associated with the socioeconomic status in the neighboring regions.

$$I_B\left(\frac{n}{\sum_{i=1}^{n}\sum_{j=1}^{n} w_{ij}}\right)\left(\frac{\sum_{i=1}^{n}\sum_{j=1}^{n} w_{ij}\left(x_i-\bar{x}\right)\left(y_i-\bar{y}\right)}{\sqrt{\sum_{i=1}^{n}\left(x_i-\bar{x}\right)^2\sum_{j=1}^{n}\left(y_i-\bar{y}\right)^2}}\right) \tag{5}$$

$$I_{Bi} = \frac{n\left(x_i-\bar{x}\right)}{\sum_{j=1}^{n}\left(y_i-\bar{y}\right)^2}\sum_{j=1}^{n} w_{ij}\left(y_i-\bar{y}\right) \tag{6}$$

Where I_B refers to the global bivariate Moran's I; I_{Bi} represents the local bivariate Moran's I for airport i; x_i is the amount of AEEs at airport i ;x_i is the amount of AEEs at airport i and $\bar{x}$ is the average amount of AEEs; y_i is the value of the socioeconomic factors at city j and y is the average amount of them.

Results and discussions

Analysis of the relative change

The COVID-19 pandemic has inflicted a heavy toll on the civil aviation industry, but it has also eased the environmental pressure on airports in 2020. Table 3 shows the descriptive statistics of EQ and EI at 22 airports in the YRD. Figure 2 shows the spatial distribution of relative changes

Table 3 Descriptive statistics of EQ and EI at 22 airports, YRD

	Type	Period	Min	Max	Mean	St.d
Emission Quantity (t)	HC	2020	1.12	97.30	17.28	26.59
		2019	1.21	167.44	23.93	41.15
	CO	2020	16.17	1583.54	274.28	408.52
		2019	21.57	2391.33	341.84	567.69
	NO_x	2020	19.76	2578.96	468.22	716.84
		2019	32.68	4195.48	614.39	1043.37
Emission Intensity (g/pax)	HC	2020	1.49	5.48	2.55	1.00
		2019	0.97	3.39	2.00	0.52
	CO	2020	30.62	73.51	40.58	10.44
		2019	25.02	41.27	30.42	4.52
	NO_x	2020	50.64	89.80	64.40	12.04
		2019	40.11	68.84	51.19	7.61

in EQ and EI at each airport between 2020 and 2019.With the Jenks natural breaks optimization method, the relative changes were classified into 5 degrees and represented by different cycle sizes in Fig. 2. Such a classification method can ensure that the features are divided into classes whose boundaries are set where there are relatively big differences in the data values. Overall, it is evident that there is a decline in EQ of the studied AEEs at all airports. The relative change of EQ ranges from − 47.7 to − 1.13% for HC, − 35.79 to − 0.79% for CO and − 39.55 to − 1.57% for NO_x. In general, the EQ emitted at airports in Shanghai, western Jiangsu province, and southern Anhui province decreased more significantly in 2020, indicating that the civil aviation industry in these regions has suffered a greater blow than other regions in the YRD. In contrast, there was an increase in EI at all airports in the YRD, especially for airports located in the middle and southern parts of Zhejiang province and Jiangsu province, southern Anhui province, and Shanghai. Given that the aircraft types on certain routes connecting the airports in the YRD barely changed in 2020 compared to 2019, the impact of aircraft type on the EI could be ignored. The EI of a trip strongly depends on the passenger load factor (Dhital et al. 2022). Defined by the ratio of the passengers onboard to the total number of available seats, the passenger load factor measures how much of the passenger carrying capacity is used. The significant rise in EI at all airports in the YRD indicated the decline in the load factor of passengers during the COVID-19 pandemic, which can be explained by the following two reasons: (i) the collapse in air travel demand caused an oversupply of seats on flights. And it has been reported that some airlines were flying essentially empty aircraft to avoid losing their slots at slot-constrained airports (Sun et al. 2021); (ii) to limit the "touchpoint" opportunities for COVID-19 to spread via close physical proximity between passengers on flights, the CAAC urged that airlines should ensure social distancing when assigning seats onboard in 2020. Therefore, it can be inferred that the decline in the aircraft occupancy rate significantly contributes to EI growth.

To study how the COVID-19 pandemic affected the AEEs at airports in the YRD, we further analyzed the relationship between the spread of COVID-19 and the monthly variation of relative changes in the AEEs. Policy responses to the pandemic are also taken into consideration. Figure 3 shows the relative changes in EQ and the number of newly confirmed cases in 2020. Figure 4 demonstrates the daily difference in the new confirmed cases, existing confirmed cases of COVID-19, and the total confirmed cases between different cities in the research region.

In the YRD, the first confirmed case of COVID-19 was identified in Shanghai on January 20, 2020. Three days later, infections were reported in all provinces of the YRD. At the same time, all regions in the YRD have initiated the highest level of public health emergency responses. The number of daily new cases gradually climbed and peaked during late January and early February. And numerous flights were canceled due to the vigorous restrictions on air transportation services. Consequently, the Chinese New Year Festival (CNYF) of 2020 (from January 24 to February 8) witnessed a sharp decline in flights and the AEEs at all airports in the YRD. The decline was unprecedentedly significant in February as the CNYF was usually a peak season for air traffic. Compared to the same period in 2019, the average EQ of HC, CO, and NO_x at airports in the YRD decreased by 30.16%, 16.68%, and 40.66%, respectively. However, as the number of new cases turned zero in the YRD by the end of February, the travel restrictions have been slightly relaxed. Different neighborhoods and townships are categorized into high, medium, or low risk, depending on the number of confirmed cases and whether there are cluster cases, which formed the basis for the gradual easing of lockdown measures. This policy also led to the rise of the AEEs at some airports in the study area since March.

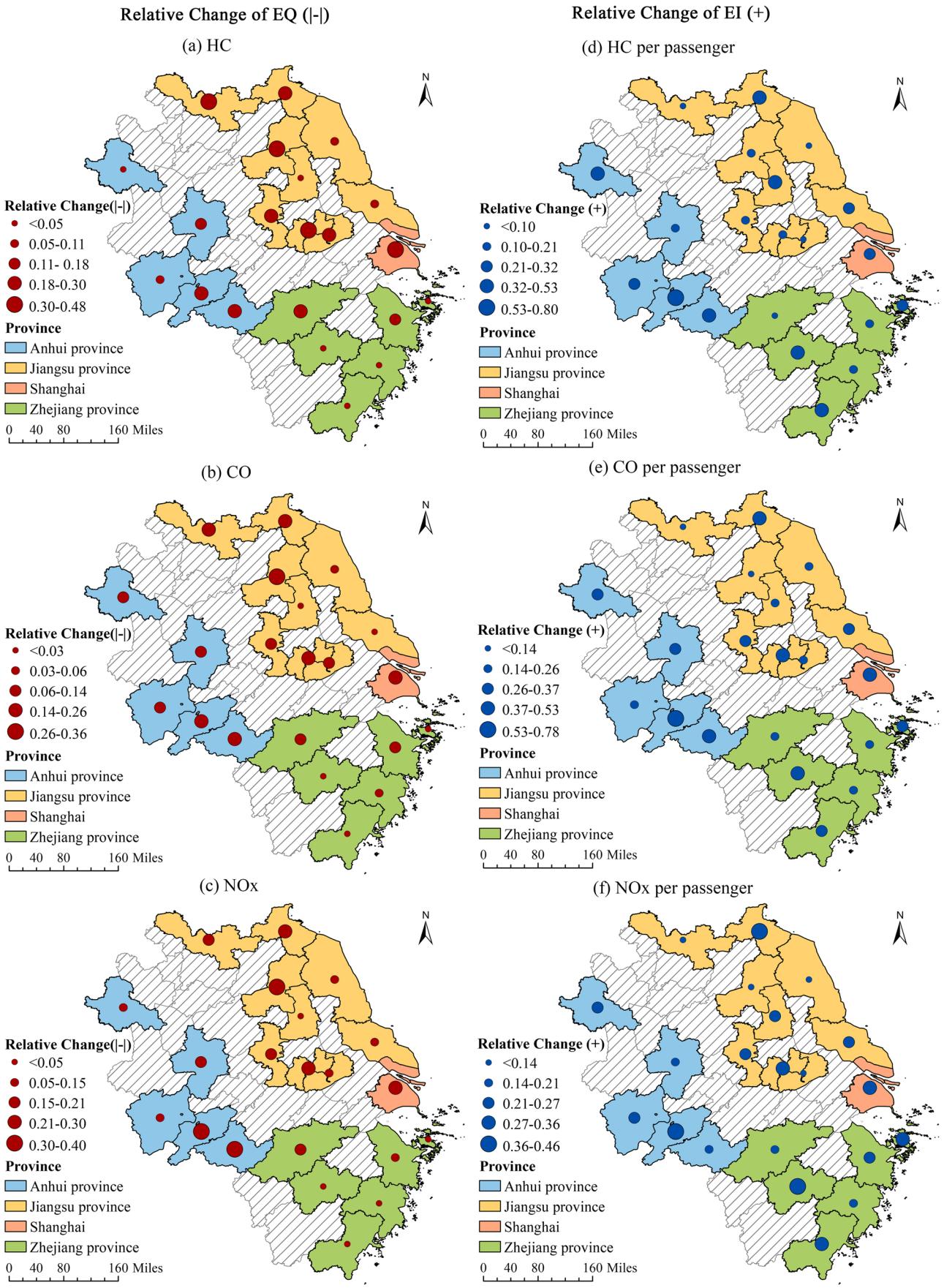
Relative Change of EQ (|-|)
(a) HC
Relative Change(|-|)
<0.05
0.05-0.11
0.11- 0.18
0.18-0.30
0.30-0.48
Province
Anhui province
Jiangsu province
Shanghai
Zhejiang province
0 40 80 160 Miles
N
(b) CO
Relative Change(|-|)
<0.03
0.03-0.06
0.06-0.14
0.14-0.26
0.26-0.36
Province
Anhui province
Jiangsu province
Shanghai
Zhejiang province
0 40 80 160 Miles
N
(c) NOx
Relative Change(|-|)
<0.05
0.05-0.15
0.15-0.21
0.21-0.30
0.30-0.40
Province
Anhui province
Jiangsu province
Shanghai
Zhejiang province
0 40 80 160 Miles
N
Relative Change of EI (+)
(d) HC per passenger
Relative Change (+)
<0.10
0.10-0.21
0.21-0.32
0.32-0.53
0.53-0.80
Province
Anhui province
Jiangsu province
Shanghai
Zhejiang province
0 40 80 160 Miles
N
(e) CO per passenger
Relative Change (+)
<0.14
0.14-0.26
0.26-0.37
0.37-0.53
0.53-0.78
Province
Anhui province
Jiangsu province
Shanghai
Zhejiang province
0 40 80 160 Miles
N
(f) NOx per passenger
Relative Change (+)
<0.14
0.14-0.21
0.21-0.27
0.27-0.36
0.36-0.46
Province
Anhui province
Jiangsu province
Shanghai
Zhejiang province
0 40 80 160 Miles
N

◂**Fig. 2** Spatial distribution of relative changes between 2020 and 2019 in EQ and EI. a Absolute of relative changes of the EQ of HC; b absolute of relative changes of the EQ of CO; c absolute of relative changes of the EQ of NOx; d relative changes of EI of HC; e relative changes of EI of CO; f relative changes of EI of NOx

To resolutely contain the increasing risks of imported COVID-19 cases, the information on international flight plans (Phase Five) was released by the Civil Aviation Administration of China (CAAC) on March 12. Two weeks after, notice on further reducing international flights was issued by CAAC. But, still, foreign-imported infections began to account for almost all the resurgence of COVID-19 cases in Shanghai, which made Shanghai the city with the most infections in the research region in 2020. Because of the restricted quarantine policies for the inbound passengers, Shanghai successfully prevented new cases from spreading exponentially in 2020. On April 30, there were no existing infections in the three provinces, indicating that the COVID-19 pandemic had been successfully controlled in the YRD by the end of April. At that time, the relative change of the EQ began to rebound. The post-pandemic reopening of the economy has again boosted the demand for domestic air travel, which significantly offset the reduction in international flights. As a result, the next 2 months witnessed a considerable increase in the AEEs at most airports in the YRD. During the second half of 2020, airlines in China have been restoring flights and regaining passengers for domestic services. The reviving domestic business has slightly boosted the local civil aviation industry. In September, there was a drastic growth in the AEEs. And, for the first time in 2020, the emissions of the studied AEEs surpassed the values in the same period in 2019. The EQ of AEEs continued to climb, and the relative change peaked at around 20% in October, when people in China enjoyed 10 days off to celebrate the National Day and Mid-Autumn Festival. The public holidays stimulated the tourism market, which, in turn, boosted the demand for air transportation. Thus, the amount of AEEs at airports became relatively higher in October, with an average change of 14.43% for HC, 19.49% for CO, and 21.71% for NO_x, respectively. However, as the weather turned colder in November and December, the relative change of the three types of AEEs plummeted again because of a growing public fear of COVID-19 infection.

Classification of temporal variation patterns

The EQ of AEEs at different airports experienced different variation patterns in the year 2020. According to the results obtained from the modified k-means clustering algorithm, some common shapes can be used to illustrate the variation patterns of the AEEs during the first half of 2020, including the shape of letters "W," "U," and "V." Fig. 5 shows the classification result of CO for the first half of 2020 (from January to June). And these classification results are similar for the other two AEEs as well.

A W-shaped pattern refers to the type of variation that resembles the letter "W" when charted. The W-shaped variation pattern of AEEs at an airport indicated that the civil aviation industry in that region began to recover rapidly after the significant decrease during the most challenging period of the COVID-19 pandemic but then turned down into another decline. Such a double-dip variation pattern may exhibit a false sign of recovery at first, but the industry just crashed again in the second round. Four airports are categorized into the W-shape, and three (FUG, AQG, and JUH) experienced a second decline in May, followed by another increase in June (43.88%, 54.99%, and 50.16%, respectively). According to CAAC (2015), the four airports in this category (i.e., HYN, FUG, AQG, and JUH) are all small branch-line airports that serve only domestic and intra-provincial flights, and their annual passenger throughput is less than 2 million. Another similarity is that these airports have a larger portion of tourist traffic as they are in cities with proximity to tourist attractions. Therefore, they are relatively less resilient in the face of the pandemic disruption compared to the airports that serve a large proportion of business passengers who travel regularly. That may explain why these airports show a fluctuated variation of AEEs during the first half of 2020.

A U-shaped pattern refers to the type of variation that takes on the shape of the letter "U" when charted. A U-shaped pattern, in this case, presents that the AEEs at these airports did not begin to increase until April at the earliest, even though the coronavirus cases in the YRD are under control in March and the economies began to be reopened. Airports that experienced a U-shaped variation pattern include two hub airports (SHA and PVG) located in Shanghai with dense international and domestic routes and two mainline airports located at the capital city (NKG and HGH). However, there still exists some disparity in the variations, even for the airports classified in the same category. For example, the growth of AEEs at PVG in May is much smaller than the other U-shaped airports, with an increase of only 23.16% for HC, 12.92% for CO, and 28.38% for NO_x. In contrast, the average growth of AEEs at other airports is 43.01% for HC, 37.93% for CO, and 42.04% for NO_x. Such disparity is associated with the difference in the functional positions of the airports. As one of the major aviation hubs of East Asia, PVG handles a larger proportion of international flights. In comparison, other airports mainly serve domestic and regional flights. After the five international flight plans (phase five) issued by CAAC, the number of international routes and inbound flights from other nations slumped to an unprecedented low level that has not been experienced for years. And this could explain the more minor increase in AEEs from PVG compared to other airports.

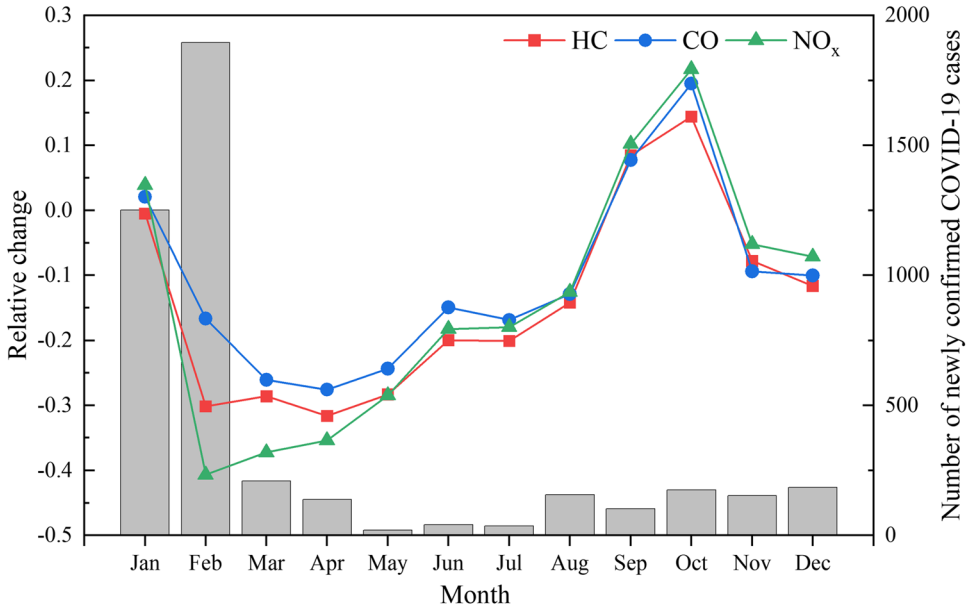

Fig. 3 Relative changes in EQ of the AEEs between 2019 and 2020, and the number of newly confirmed cases in 2020

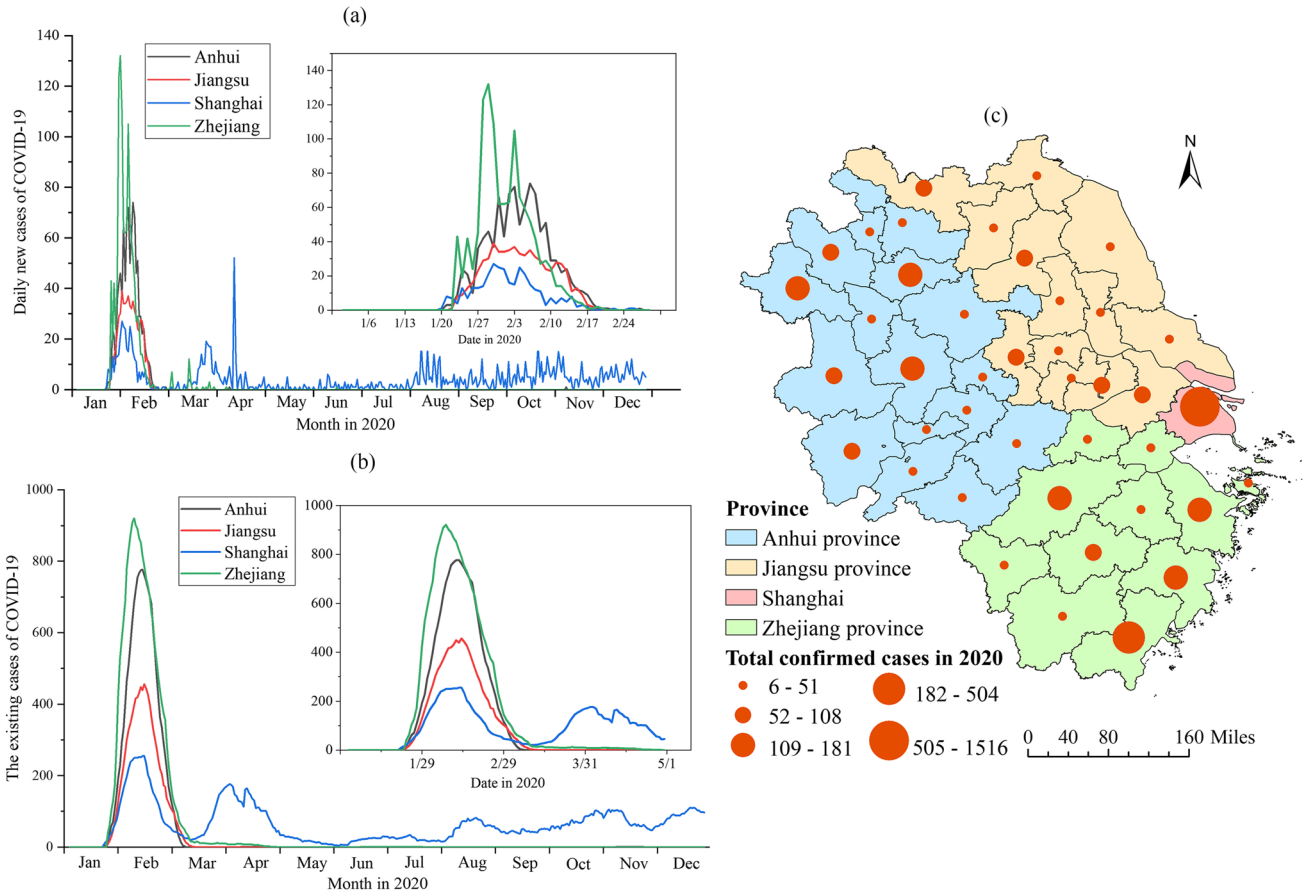

Fig. 4 The COVID-19 situation in the YRD, 2020. a Daily new cases of COVID-19 at each province and Shanghai in the YRD, 2020. b The existing cases of COVID-19 at each province and Shanghai in the YRD, 2020. c The total confirmed case at each city in the YRD, 2020

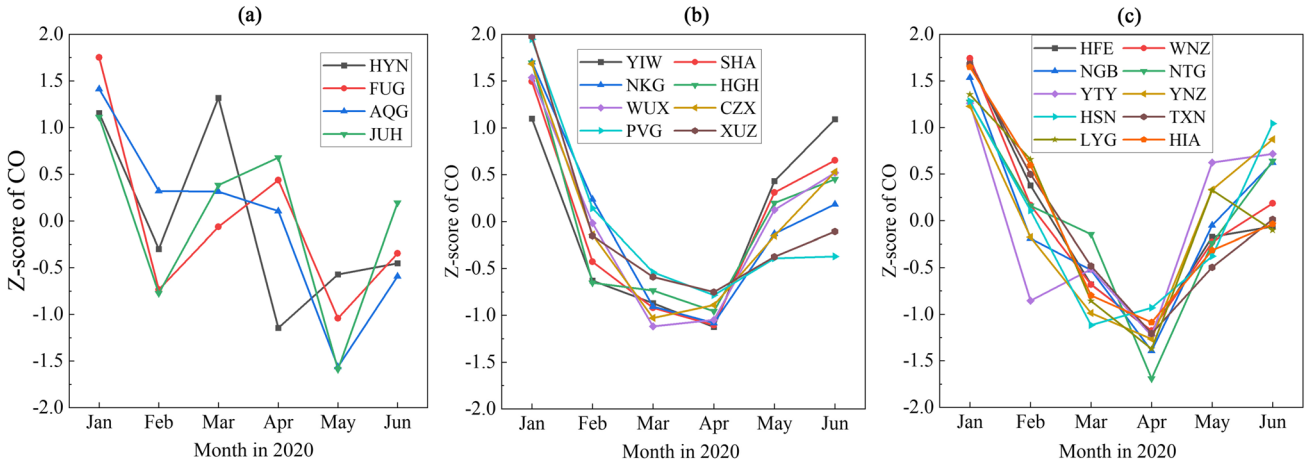

Fig. 5 The classification results of variation patterns during the first half of 2020. **a** The W-shaped variation patterns of CO; **b** the U-shaped variation patterns of CO; **c** the V-shaped variation patterns of CO

A V-shaped pattern refers to the type of variation that resembles the letter "V." Nearly half of the airports in the YRD exhibited a V-shaped variation pattern, which was characterized by a quick and sustained increase after the continuous sharp declines in the AEEs. However, for most airports, the variation of AEEs did not always follow a full V-shape, because it was extremely difficult for the right side to peak at the pre-crisis level in such a short time, considering the huge recession that aviation suffered from the COVID-19 pandemic. The greatest difference between V-shaped and U-shaped patterns is that a V-shaped variation does not bump along the bottom. Airports that experienced a V-shaped variation pattern include 5 airports in Jiangsu province, 3 airports in Zhejiang province, and 2 airports in Anhui province. Except for HFE, all the airports that are classified into this category are medium-sized airports located in non-capital cities of the provinces. The strength of the recovery in one certain area is closely associated with the severity of the preceding impact of COVID-19, as well as the airport's resilience to severe events. For most of the airports, the continuous downward trend ends in April.

The control of the COVID-19 pandemic allowed the recovery of domestic air transportation at most of the airports in the YRD during the second half of 2020. The increasing confidence in air travel also resulted in an upsurge in the AEEs. Generally, there are three types of tendencies for the variation patterns of AEEs in the second half of 2020: upward trend, fluctuation, and downward trend. Figure 6 shows the classification result of CO for the second half of 2020 (from July to December). And this classification result holds true for the other two AEEs as well.

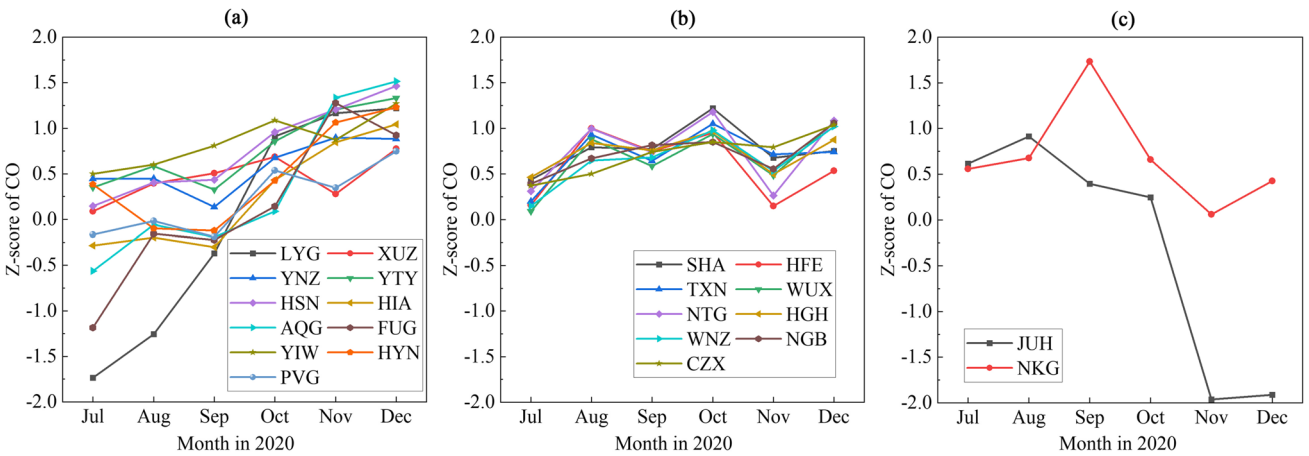

Fig. 6 The classification results of variation patterns during the second half of 2020. **a** The variation patterns of CO with an upward trend; **b** the variation patterns of CO with a fluctuated trend; **c** the variation patterns of CO with a downward trend

Airports that presented an upward trend of the variation patterns of the AEEs are small airports (except for PVG) with relatively fewer annual flights in the YRD. The marked surge of AEEs at these airports indicated that smaller airports in the research region were more resilient to the COVID-19 pandemic. As for airports that presented a fluctuation trend, almost all these airports experienced some levels of increase in the AEEs in August 2020. The increase ranged from 8.61 to 45.58% for HC, 4.48 to 33.64% for CO, and 11.58 to 41.3% for NO_x, indicating a further recovery of civil aviation in most areas of the research region. From August to December, the amount of AEEs from LTO cycles at these airports slightly fluctuates around the same level as July (the change ranges from – 20 to 20%). And airports that witnessed this type of variation trend are usually intermediate or large airports that are busy for the whole year. In comparison, airports that experienced greater changes are smaller airports (e.g., AQG, JUH, LYG, HIA, and FUG) that relied greatly on the local tourism industry. As for these airports, there are sharp rises in the amount of AEEs in the peak season of tourism and declines in the off-season of tourism. As can be seen in Fig. 6 (c), only JUH and NKG witnessed downward trends of AEEs. JUH was specially built to serve tourists who come to visit Jiuhua Mountain. Because November is one of the worst seasons to travel to Jiuhua Mountain, it is reasonable that the AEEs plummet at that time. As for NKG, the variation patterns of the AEEs experienced a noticeable rise in September, followed by a significant decline in October. Such a phenomenon may be explained by the fact that Nanjing is one of the cities with the most universities and institutes in China. Given that September is the beginning of a new semester, numerous students flied to Nanjing from all over the country at this time, which contributed to the sharp rise in AEEs in September 2020.

Table 4 Univariate global Moran's I

	Variable	Global Moran's I
EQ of AEE	HC	0.155841**
	CO	0.125544***
	NO_x	0.169038**
EI of AEE	HC	0.128533***
	CO	0.119157**
	NO_x	0.110603***
Economic indicator	GDP	0.291022*
	GDP per capita	0.579645**
Demographic indicator	Population	0.144057*
	Population density	0.276255**

*Statistically significant at the 10% level; **significant at the 5% level; ***significant at the 1% level.

Spatial dependence analysis

Spatial autocorrelation analysis

Table 4 shows that the global Moran's I of EQ, EI, and other socioeconomic factors (i.e., GDP, GDP per capita, population, and population density) are all greater than 0, indicating the presence of positive spatial autocorrelation in the YRD. The Moran's I of the AEEs is relatively lower compared to the Moran's I of these socioeconomic indicators. Several reasons may account for this. Firstly, affected by the localized management mechanism of air transportation, the distribution of resources for airports is uneven. For instance, the government of Jiangsu province established the China East Airport Group (EAG) in 2018, which is responsible for the general planning and co-construction of all airports in Jiangsu province except for WUX and NTG. Accordingly, there still exists a large gap between the development of civil aviation in different cities. Some airports received more investments in constructing airport facilities than their neighbors, leading to significant unbalanced development within the studied region. Secondly, the YRD has a well-developed expressway network and a high-speed railway network. As of the end of 2019, 20 high-speed rail lines have opened in the region, making the YRD the region with the highest density of high-speed rail in China. However, superior ground transportation has suppressed the interaction and coordinated development among airports in the study area. Furthermore, the aviation business in the YRD is currently highly concentrated in some major cities due to the disparity in economic development. In 2019, the passenger throughput of 8 major airports in Shanghai, Hangzhou, Nanjing, Ningbo, Wenzhou, Hefei, and Wuxi reached approximately 240 million passengers, accounting for about 90% of the total amount in the YRD. In contrast, the cumulative passenger throughput of the other 14 airports in the research region did not reach the level of 30 million passengers. Some airports are facing the problem of the saturation of operation capacity, while others are challenged by the serious shortage of business volume. The novel findings of the spatial autocorrelation analysis offered the opportunity to explore and disclose the problems behind the coordinated development of the airport group in the research region.

Figure 7 is the LISA map of EQ, which demonstrates the classification of the airports with an assessment of significance. In this case, there are three types of clustering patterns with points that are significant ($p \leq 0.05$): (1) high-high clustering (SHA and PVG)- airports with high AEEs are adjacent to airports with high AEEs; (2) low-low clustering (AQG, JUH, and TXN)- airports with low AEEs are adjacent to airports with low AEEs; (3) low–high clustering (WUX, NTG, and HSN)- airports with low AEEs are adjacent to airports with high AEEs. Generally, the

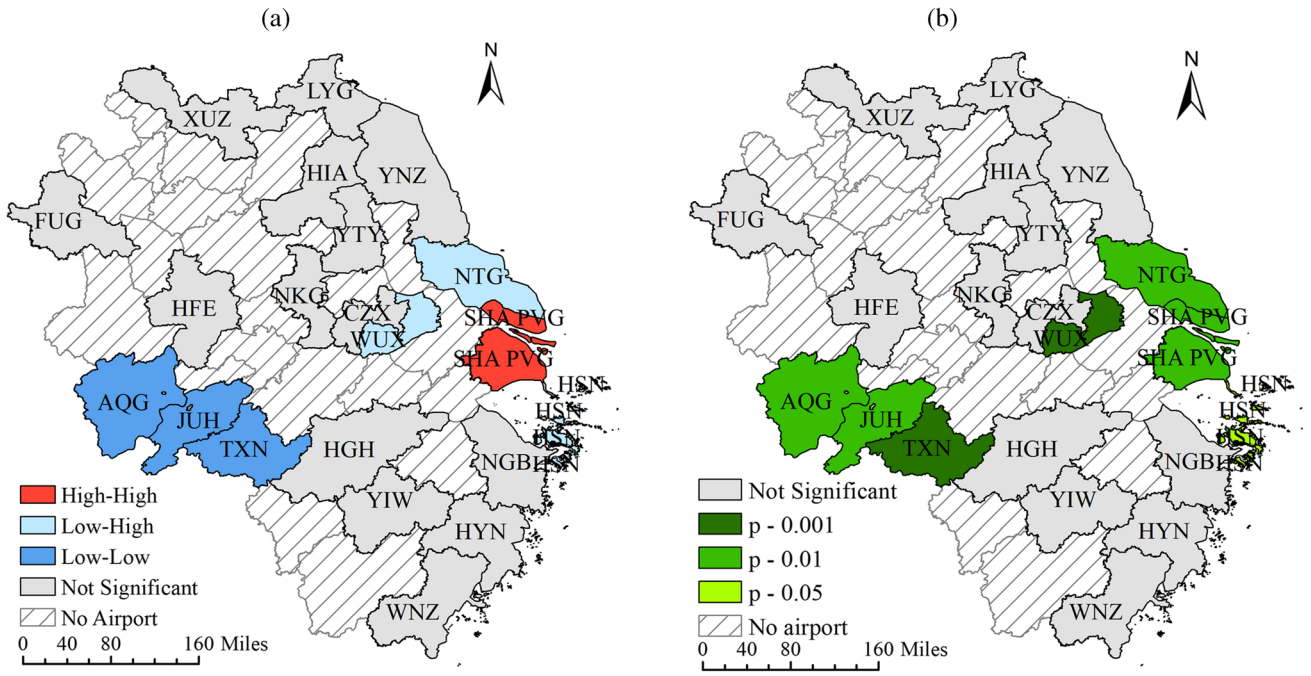

Fig. 7 The results of local spatial autocorrelation of the EQ. **a** The LISA map; **b** the significance map

high-high and low-low clustering spots, which contribute significantly to the positive global spatial autocorrelation, are polarized in the YRD. The high-high spots are distributed in the east, while the low-low spots are scattered in the west. The two airports in Shanghai belong to the high-high cluster, which indicate a great concentration of the AEEs from LTO cycles in Shanghai. The low-low cluster covers three cities in the southwest of Anhui province, suggesting a less-developed civil aviation industry across this domain. Compared to Jiangsu province and Zhejiang province, Anhui province has fewer air passenger demands, less developed airport construction, and lower airport utilization efficiency. Except for the HFE in the capital city, Hefei, which has more routes and flights, none of the airports in Anhui Province can compete with airports in Jiangsu Province. Therefore, it is reasonable that airports in the low-low cluster are in three adjacent cities in Anhui Province. The airports that belong to the low–high cluster are in Wuxi, Nantong, and Zhoushan, respectively. These cities are all close to Shanghai, which have a relatively larger population density and a higher level of economic development. Because of the high density of airports and extensive air routes in the region, the airspace and time resources of the YRD tend to be saturated (Shi et al. 2021). Airway congestion has become a prominent problem in the research region. Given the fact that Shanghai is the aviation hub in the Asia–Pacific region, the growth of air traffic in the three airports (i.e., WUX, NTG, and HSN) has been greatly suppressed to ensure the normal operation of SHA and PVG in Shanghai. The results of local spatial autocorrelation of the EI with an assessment of significance are presented in Fig. 8. It is noteworthy that airports located in southern Anhui province (i.e., AQG, JUH, and TXN) are categorized as high-high clusters, whereas airports located in the southeast Zhejiang province are identified as low-low clusters. One of the primary causes that may explain this result may be the economies of scale, as the converted throughput per airport in southeast Zhejiang province was much higher than in southern Anhui province.

Spatial association analysis

The bivariate Moran's I model is used to address the closely pertinent question: is there any spatial correlation between AEEs and other socioeconomic factors? Table 5 shows the bivariate Moran's I statistics and the corresponding *p*-values. The values of bivariate Moran's I show that GDP, GDP per capita, population, and population density are all spatially correlated with AEEs at airports in a positive way. And the interactions of those factors between the cities with closer geographic positions are relatively significant (all Moran's I values > 0, *p*-values ≤ 0.05). An increase in any of these socioeconomic factors would promote the corresponding AEEs at airports for other cities that were geographically nearby at the same time. This result is consistent with extensive literature, which argues that socioeconomic factors have always been the important driving force for the aviation sector (Wang et al. 2020; Liu et al 2021). The strongest

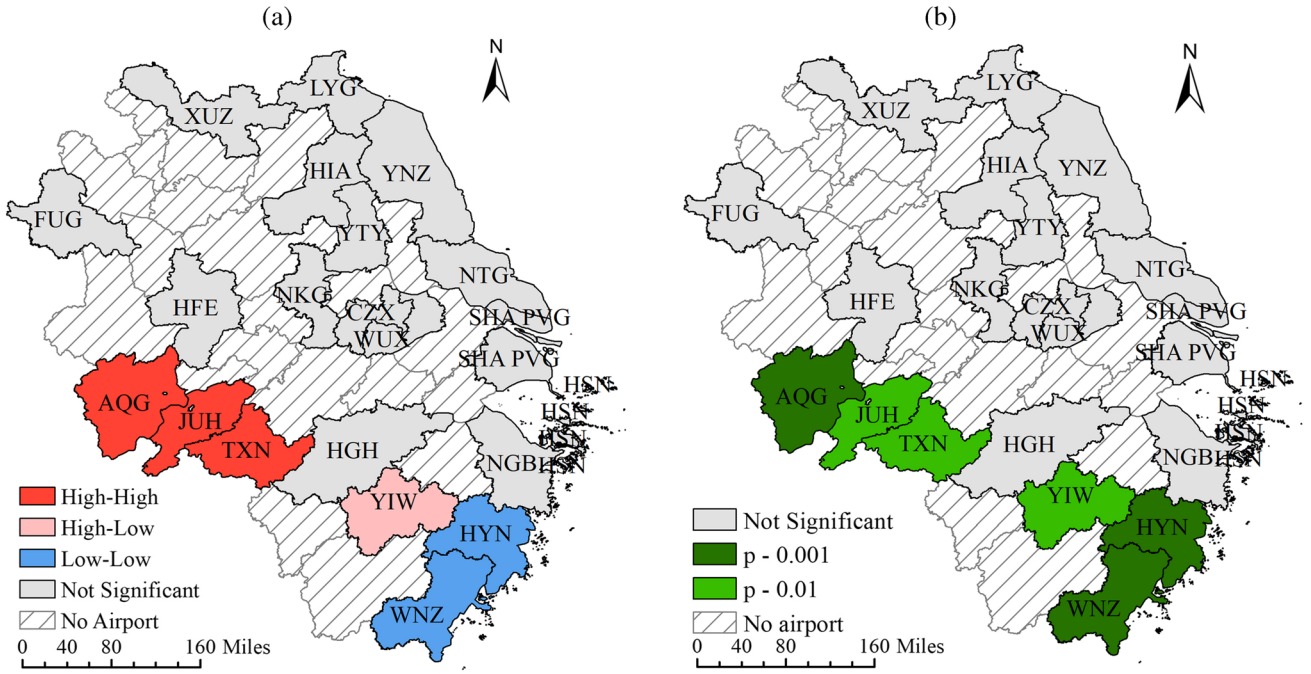

Fig. 8 The results of local spatial autocorrelation of the EI. **a** The LISA map; **b** the significance map

Table 5 Bivariate global Moran's I in the YRD

First variable (*X*)	Second variable (*Y*)	Moran's I
HC	GDP	0.244632**
CO	GDP	0.231359**
NO_x	GDP	0.248902**
HC	GDP per capita	0.406193***
CO	GDP per capita	0.396324***
NO_x	GDP per capita	0.409726***
HC	Population	0.163799*
CO	Population	0.154004*
NO_x	Population	0.167640*
HC	Population density	0.242420**
CO	Population density	0.239702*
NO_x	Population density	0.247184**

*Statistically significant at the 10% level; **significant at the 5% level; ***significant at the 1% level.

spatial correlation is observed between the AEEs and GDP per capita (mean Moran's I: 0.404), suggesting that the higher the economic welfare and living standard is in the neighboring region, the larger amount of AEEs at local airports is likely to be generated. This situation is probably due to the mutually supportive relationship between the local economy and the civil aviation industry (Addepalli et al. 2018). Generally, the contribution of air transport and related civil aviation industries to local economies includes the output and jobs directly attributable to civil aviation, as well as the multiplier or ripple effect upon other industries throughout the economy. Meanwhile, the local economy contributes to the aviation industry by boosting passenger demand for the transport of passengers, mail, freight, and other services. Since AEEs from LTO cycles are highly reliant on flight demand, the strong positive spatial relationship between AEEs and local economic conditions is, therefore, reasonable.

The Bi-LISA cluster map (Fig. 9) depicts the spatial clustering and spatial outliers of the studied AEEs by the lagged values of GDP per capita, GDP, population, and population density. Similar to the univariate LISA map mentioned above, it can be observed that AQG, JUH, and TXN also appeared in the low-low region on all the Bi-LISA cluster maps, indicating that the three airports, which have a relatively smaller amount of AEEs, are surrounded by cities with poorer economic performance, smaller population, and smaller population density. Being the financial center of the YRD, the two airports in Shanghai are again identified as the significant high-high region, which is consistent with the fact that Shanghai has apparent economic externalities and a spatial spillover effect on its neighboring cities in terms of many socioeconomic aspects. Besides, slight differences can be found between the clustering patterns of GDP and per capita GDP. On the Bi-LISA map for the AEEs and GDP per capita, more spatial units are included in the

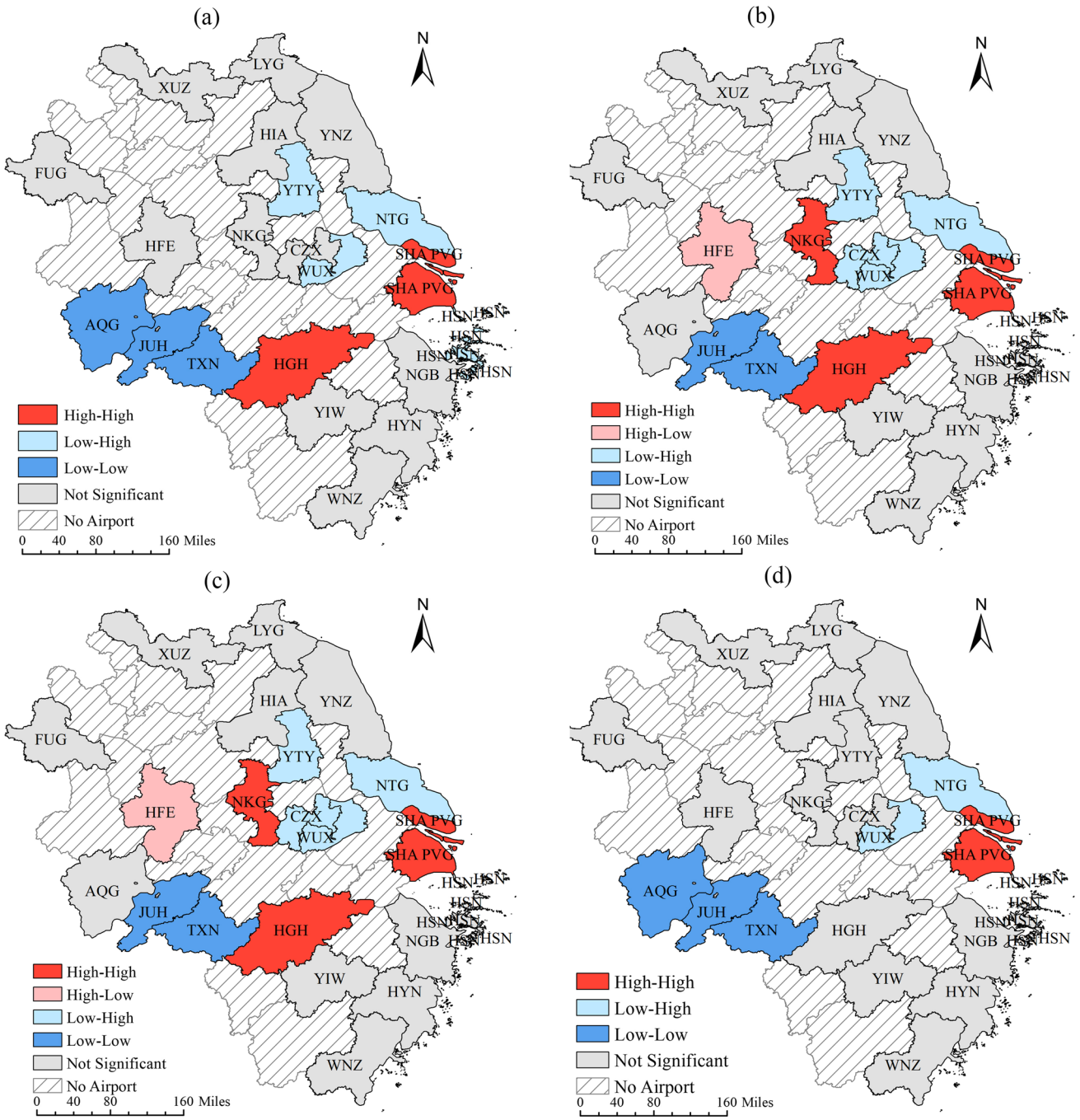

Fig. 9 The bivariate LISA map for the YRD. **a** AEEs and GDP; **b** AEEs and GDP per capita; **c** AEEs and population; **d** AEEs and population density

high-high and low–high regions. NKG is identified as a high-high cluster, indicating that NKG has AEEs more than the average amount, and the contiguous cities also present a higher per capita GDP value than the average. In contrast, NKG is not significant on the Bi-LISA mapr for the AEEs and GDP. Besides, except for WUX and NTG, CZX and YTY are also classified as the low–high spatial outliers when using per capita GDP as the second variable. This can be explained by the fact that these airports are all close to the airports classified as high-high clusters. The Bi-LISA maps for the AEEs and population and population density present the same distribution pattern. In general, regions predominantly from the west of the YRD are relatively less developed in terms of civil aviation and other socioeconomic aspects, which, in turn, resulted in fewer AEEs released from LTO cycles.

Policy implications

Based on the results and discussion above, we provide recommendations for building a more sustainable and environment-friendly airport group in the YRD.

Reducing the aircraft taxiing time with integrated methods

The air pollutant emissions released during a typical LTO cycle are closely related to the time spent in each mode of the operation (i.e., idle, approach, takeoff, and climb out). From the perspective of the airport authorities, the most feasible way to cut the AEEs at the ground level is to reduce the operation time of the aircraft at the airport. Previous studies have suggested that the taxi mode of the aircraft contributes the biggest portion of the total LTO emissions (Song and Shon 2012; Yılmaz 2017). It has also been estimated that fuel burned during taxiing accounts for up to 6% of the total fuel consumption by an airline fleet for short-haul flights (Brownlee et al. 2018), and a shorter taxiing time can potentially save one-third of the fuel (Hao et al. 2017). Therefore, reducing the aircraft taxiing time should be considered a critical issue in alleviating aircraft emissions at airports. With this aim, the optimization of the ground movement of aircraft on the taxiway has been the focus of extensive studies over the past decades, which involves the routing problems and the scheduling problems (Adacher et al. 2018). With the development of computer science, different algorithms are capable of solving the problems, such as the adapted heuristic algorithm (Zhang et al. 2018) and modified Dijkstra's short-path algorithms (Brownlee et al. 2018). Some other integrated approaches to optimizing the ground movement of aircraft include optimizing gate allocation (Chow et al. 2022; Jiang et al. 2022a, b) and runway sequencing (Jiang et al. 2022a, b). In addition, potential approaches to increase the taxi efficiency of the aircraft may include increasing the airport capacity, using more advanced automation and information management system to improve the performance of air traffic control (ATC) and so forth. By adopting these approaches at the airports, the idling time of aircraft on the taxiway can be minimized, and, thus, the pollutant emissions from aircraft at ground levels can be hopefully reduced.

Improving demand management and air traffic management

The occurrence of severe public emergencies, such as COVID-19, led to unpredictable fluctuations in the demand for air transportation. The plunge in air passengers, as well as the stringent social distancing standards during flights, has forced the airlines to cut down the seating capacity, which consequently resulted in the surge of emission intensity per passenger at the airports. Traditionally, each air route is designated with a certain type of aircraft based on the historical average demand. However, this strategy does not fit the ever-changing civil aviation market. During the post-COVID-19 era, airlines should be encouraged to enhance the ability to predict passenger demand and increase the flexibility when assigning aircraft to a specific route to avoid the huge oversupply of seats onboard. It would be more environment-friendly so that the capacity of the designated aircraft can better match the demands of specific air routes. Furthermore, the ever-changing air traffic level during the COVID-19 pandemic has also brought great challenges to air traffic management (ATM), as the system and air traffic controllers had to respond quickly to variable situations and simultaneously maintain efficiency and performance. Previous studies have argued that the performance of air traffic controllers was negatively impacted by the COVID-19 pandemic, leading to rising concerns about longer flight delays and more aircraft emissions (Vink 2021). Hopefully, the application of advanced air traffic management technologies may greatly reduce human errors and provide tactical decision support (Xue et al. 2021a). Aiming at increasing flight efficiency, ICAO has been proposing the Communication, Navigation, and Surveillance for ATM (CNS/ATM) (2). As a key component, the Automatic Dependent Surveillance-Broadcast (ADS-B) can offer accurate and reliable real-time aircraft positions (Xue et al. 2021a) and, thus, improve ATM efficiency. Besides, switching the traditional ground navigation system to a satellite navigation system should be encouraged to strike a balance between flight demands and airport capacity (Xue et al. 2022). In addition, the arrival manager (AMAN) and the departure manager (DMAN) are useful sequencing tools that can help air traffic controllers to improve their situational awareness and to anticipate the flow of traffic (Insaurralde and Blasch 2022). The adoption of coupled AMAN-DMAN allows for optimization of the arrival and departure sequence, and, thus, helps ensure efficient demand coordination and reduce the fuel burn of aircraft (Liang et al. 2018). Other technologies that can be adopted by the airport to improve ATM and reduce the AEEs include terminal flight data manager (TFDM), airport surveillance radar (ASR-11), trajectory-based operations (TBO), and so forth. By improving demand management and air traffic management, airports and airlines would be able to look beyond the pandemic and adapt to the long-term realities of COVID-19.

Enhancing coordinated development of civil aviation in the YRD

The development of civil aviation in the YRD is highly unbalanced, which can be reflected by the spatial clustering patterns of the AEEs at airports in the YRD. Currently, a great number of airports in the YRD are challenged by a shortage of flights, while airports in megacities (e.g., Shanghai, Hangzhou, Nanjing) are facing severe problems of capacity saturation. Consequently, extensive delays and longer operation time on the ground are caused by capacity saturation, resulting in the escalation of air pollutant emissions from the aircraft. Therefore, airports with larger traffic need to make better use of airport resources and improve the ability to manage airflow so that emissions caused by congestion and delays can be reduced. Besides, communication and cooperation between different airports should also be encouraged as the shared information is beneficial for building a more sustainable airport group. In addition, the regional government should be encouraged to seek a balance between unified management strategies and differentiated policies based on the functional position of the airports and the according local development characteristics. The recommendations above for building a more sustainable airport group can all be achieved by implementing collaborative decision making (CDM). As a joint government and industry initiative, CDM aims to improve traffic flow and capacity management performance by encouraging different aviation stakeholders to work together and make decisions based on shared information (Corrigan et al. 2015). The successful implementation of CDM at many airports in the world has proved its advantages in improving the efficiency and quality of airport operation, assisting the decision-making process of aviation community stakeholders, and enhancing the collaboration between different aviation stakeholders (Okwir et al. 2017).

Conclusions

The dramatic drop in the demand for air travel, together with the traffic restrictions, led to the decline in AEEs from LTO cycles at airports. Compared to 2019, the EQ of HC, CO, and NO_x decreased greatly at airports in the YRD in 2020. However, there was a significant rise in the EI, mainly due to the decline of passenger load factors during the COVID-19 pandemic. The temporal variation patterns of the studied AEEs were significantly influenced by the policy responses to the epidemic and the severity of the COVID-19. The monthly variation pattern of the AEEs during the first half of 2020 was classified into W-shaped, U-shaped, and V-shaped patterns. During the second half of 2020, three types of tendencies for the variation patterns were observed, including upward trend, fluctuation, and downward trend. The positive spatial autocorrelation was found in both the EQ and EI of AEEs at airports in the YRD. As for EQ, the high-high cluster and low-low clusters were polarized in the YRD. The high-high cluster was located in the east, while the low-low cluster was located in the west. As for EI, airports distributed in the southern YRD presented stronger spatial dependence. The positive spatial association was found between the AEEs and the external socioeconomic factors (i.e., GDP, GDP per capita, population, and population density) of the cities in close proximity. The strongest spatial association was observed between the AEEs and GDP per capita, indicating that the higher the economic welfare and living standard is in the neighboring, the more AEEs from LTO cycles are likely to be generated.

Several limitations exist in this study. Firstly, it should be noted that the engine performance can be affected by airport meteorological conditions. Therefore, it would be valuable to include the meteorological factor when calculating the amount AEEs in the future. Moreover, due to limited data access and permission, this research only took the Yangtze River Delta located in central eastern China as an example to study the variations of AEEs and their relationship with other external factors. Further research can expand the study area to the whole nation and other countries.

Author contribution DB: conceptualization, funding acquisition, methodology, formal analysis, writing—original draft, resources, and supervision. ST: conceptualization, funding acquisition, methodology, formal analysis, and writing—original draft. DK: writing, review, editing, and supervision. ZZ: data curation. TZ: visualization.

Funding This work was supported by the Fundamental Research Funds for the Central Universities, (NO. NS2020047) and the Foundation of the Graduate Innovation Center, Nanjing University of Aeronautics and Astronautics (NO. xcxjh20210705).

Data availability The datasets generated and analyzed during the current study are available from the corresponding author on reasonable request.

Declarations

Ethics approval Not applicable.

Consent to participate Not applicable.

Consent for publication Not applicable.

Competing interests The authors declare no competing interests.

References

Adacher L, Flamini M, Romano E (2018) Airport ground movement problem: minimization of delay and pollution emission. IEEE Trans Intell Transp Syst 19(12):3830–3839. https://doi.org/10.1109/TITS.2017.2788798

Addepalli S, Pagalday G, Salonitis K, Roy R (2018) Socioeconomic and demographic factors that contribute to the growth of the civil aviation industry. Procedia Manuf 19:2–9. https://doi.org/10.1016/j.promfg.2018.01.002

Adrienne N, Budd L, Ison S (2020) Grounded aircraft an airfield operations perspective of the challenges of resuming flights post COVID. J Air Transp Manag. https://doi.org/10.1016/j.jairtraman.2020.101921

Amato F, Moreno T, Pandolfi M, Querol X, Alastuey A, DelgadoA PM, Cots N (2010) Concentrations, sources and geochemistry of airborne particulate matter at a major European airport. J Environ Monit 12(4):854–862. https://doi.org/10.1039/B925439K

Anselin L (1995) Local indicators of spatial association—LISA. Geogr Anal 27(2):93–115. https://doi.org/10.1111/j.1538-4632.1995.tb00338.x

Ashok A, Balakrishnan H, Barrett SR (2017) Reducing the air quality and CO2 climate impacts of taxi and takeoff operations at airports. Transp Res Part d: Transp Environ 54:287–303. https://doi.org/10.1016/j.trd.2017.05.013

Aygun H, Caliskan H (2021) Environmental and enviroeconomic analyses of two different turbofan engine families considering landing and take-off (LTO) cycle and global warming potential (GWP) approach. Energy Convers Manag 248:114797

Bao D, Tian S, Zhang Z, Cheng H, Zhu T, CarpeggianiN(2021) Spatial-temporal patterns of air pollutant emissions from landing and take-off cycles in the Yangtze River Delta of China during the COVID-19 outbreak. Frontiers in Public Health. https://doi.org/10.3389/fpubh.2021.673666

Brasseur GP, Gupta M, Anderson BE et al (2016) Impact of aviation on climate: FAA's aviation climate change research initiative (ACCRI) phase II. Bull Am Meteor Soc 97(4):561–583. https://doi.org/10.1175/BAMS-D-13-00089.1

Brownlee AE, Weiszer M, Chen J, Ravizza S, Woodward JR, Burke EK (2018) A fuzzy approach to addressing uncertainty in airport ground movement optimisation. Trans Res Part C: Emerg Technol 92:150–175. https://doi.org/10.1016/j.trc.2018.04.020

CAAC (2015) Civil aviation regional airport construction standards. http://www.caac.gov.cn/XXGK/XXGK/TZTG/201511/t20151105_11055.html. Accessed 21 December 2021 (in Chinese)

Cartone A, Panzera D, Postiglione P (2021) Regional economic disparities, spatial dependence and proximity structures. Regional Science Policy & Practice. https://doi.org/10.1111/rsp3.12482

Chow YT, NG KK, Keung KL (2022) An evolutionary algorithm in static airport gate assignment problem. Open Trans J 16(1). https://doi.org/10.2174/18744478-v16-e2203040

Collivignarelli MC, Abbà A, Bertanza G, Pedrazzani R, Ricciardi P, Miino MC (2020) Lockdown for COViD-2019 in Milan: what are the effects on air quality? Sci Total Environ 732:139280. https://doi.org/10.1016/j.scitotenv.2020.139280

Corrigan S, Mårtensson L, Kay A, Okwir S, Ulfvengren P, McDonald N (2015) Preparing for airport collaborative decision making (A-CDM) implementation: an evaluation and recommendations. Cogn Technol Work 17(2):207–218. https://doi.org/10.1007/s10111-014-0295-x

Cui Q, Lei Y, Li Y, Wanke PF (2022) Impacts of the COVID-19 on all aircraft emissions of international routes in South America. Iscience 25(9):104865. https://doi.org/10.1016/j.isci.2022.104865

Dhital NB, Wang LC, Yang HH, Lee CH, Shih WH, Wu CS (2022) Effects of the COVID-19 pandemic on public bus occupancy and real-world tailpipe emissions of gaseous pollutants per passenger kilometer traveled. Sustain Environ Res 32(1):1–12. https://doi.org/10.1186/s42834-022-00146-7

Dube K, Nhamo G, Chikodzi D (2021) COVID-19 pandemic and prospects for recovery of the global aviation industry. J Air Transp Manag 92:102022. https://doi.org/10.1016/j.jairtraman.2021.102022

Elias B (2020) Addressing COVID-19 pandemic impacts on civil aviation operations. Congressional Research Service. https://crsreports.congress.gov/product/pdf/R/R46483?__cf_chl_jschl_tk__=kOWD3ahI1OTw20i_s9TA5VgUI7go4GxwqUfKQuqozH0-1638758778-0-gaNycGzNCP0. Accessed 26 November 2021

Fotheringham AS, Brunsdon C (1999) Local forms of spatial analysis. Geogr Anal 31(4):340–358. https://doi.org/10.1111/j.1538-4632.1999.tb00989.x

Głowacki P, Kalina P, Kawalec M (2022) Comparing methods of calculating aircraft engine emissions of harmful exhaust components during the takeoff and landing cycle in the airspace of an airport. Trans Aerosp Res 2:62–68. https://doi.org/10.2478/tar-2022-0010

Hao L, Ryerson MS, Kang L, Hansen M (2017) Estimating fuel burn impacts of taxi-out delay with implications for gate-hold benefits. Transp Res Part c: Emerg Technol 80:454–466. https://doi.org/10.1016/j.trc.2016.05.015

Hsu HH, Adamkiewicz G, Houseman EA et al (2012) The relationship between aviation activities and ultrafine particulate matter concentrations near a mid-sized airport. Atmos Environ 50:328–337. https://doi.org/10.1016/j.atmosenv.2011.12.002

Hu R, Zhu J, Zhang Y, Zhang J, Witlox F (2020) Spatial characteristics of aircraft CO2 emissions at different airports: some evidence from China. Transp Res Part D-Transp Environ. https://doi.org/10.1016/j.trd.2020.102435

ICAO (2016) Airport local air quality guidance manual. https://www.icao.int/environmental-protection/Documents/Doc%209889.SGAR.WG2.Initial%20Update.pdf. Accessed 21 December 2021

ICAO (2020) Effects of novel coronavirus (COVID-19) on civil aviation: economic impact analysis. https://www.icao.int/sustainability/Documents/Covid-19/ICAO_coronavirus_Econ_Impact.pdf. Accessed 21 December 2021

Insaurralde CC, Blasch E (2022) Situation awareness decision support system for air traffic management using ontological reasoning. J Aerosp Inf Syst 19(3):224–245. https://doi.org/10.2514/1.I010989

Jiang Y, Hu Z, Liu Z, Zhang H (2022a) Optimization of multi-objective airport gate assignment problem: considering fairness between airlines. Transp B Transp Dynamics :1-15. https://doi.org/10.1080/21680566.2022.2056542

Jiang Y, Liu Z, Hu Z, Zhang H, Xu C (2022b) Variable neighbourhood search for the integrated runway sequencing, taxiway scheduling, and gate reassignment problem. Transportmetrica B: Transp Dynamics :1-16. https://doi.org/10.1080/21680566.2022.2127429

Ju Y, Hargreaves CA (2021) The impact of shipping CO2 emissions from marine traffic in Western Singapore Straits during COVID-19. Sci Total Environ. https://doi.org/10.1016/j.scitotenv.2021.148063

Kesgin U (2006) Aircraft emissions at Turkish airports. Energy 31(2–3):372–384. https://doi.org/10.1016/j.energy.2005.01.012

Kurniawan JS, Khardi S (2011) Comparison of methodologies estimating emissions of aircraft pollutants, environmental impact assessment around airports. Environ Impact Assess Rev 31(3):240–252. https://doi.org/10.1016/j.eiar.2010.09.001

Kuzu SL (2018) Estimation and dispersion modeling of landing and take-off (LTO) cycle emissions from Atatürk International Airport. Air Qual Atmos Health 11(2):153–161. https://doi.org/10.1007/s11869-017-0525-5

Lang F (2019) MIT study finds aviation emissions impact our air quality more than our climate. https://interestingengineering.com/mit-study-finds-aviation-emissions-impact-our-air-quality-more-than-our-climate. Accessed 12 November 2019

Lee SI (2001) Developing a bivariate spatial association measure: an integration of Pearson's r and Moran's I. J Geogr Syst 3(4):369–385. https://doi.org/10.1007/s101090100064

Lee K, Worsnop CZ, Grépin KA, Kamradt-Scott A (2020) Global coordination on cross-border travel and trade measures crucial to COVID-19 response. Lancet 395(10237):1593–1595. https://doi.org/10.1016/S0140-6736(20)31032-1

Liang M, Delahaye D, Marechal P (2018) Conflict-free arrival and departure trajectory planning for parallel runway with advanced point-merge system. Transp Res Part c: Emerg Technol 95:207–227. https://doi.org/10.1016/j.trc.2018.07.006

Linka K, Goriely A, Kuhl E (2021) Global and local mobility as a barometer for COVID-19 dynamics. Biomech Model Mechanobiol 20(2):651–669. https://doi.org/10.1007/s10237-020-01408-2

Liu A, Kim YR, O'Connell JF (2021) COVID-19 and the aviation industry: the interrelationship between the spread of the COVID-19 pandemic and the frequency of flights on the EU market. Ann Tour Res 91:103298. https://doi.org/10.1016/j.annals.2021.103298

Ma T, Hong T, Zhang H (2015) Tourism spatial spillover effects and urban economic growth. J Bus Res 68(1):74–80. https://doi.org/10.1016/j.jbusres.2014.05.005

Moran PA (1950) Notes on continuous stochastic phenomena. Biometrika 37(1/2):17–23. https://doi.org/10.2307/2332142

Musashi JP, Pramoedyo H, Fitriani R (2018) Comparison of inverse distance weighted and natural neighbor interpolation method at air temperature data in Malang region. Cauchy 5(2):48–54. https://doi.org/10.18860/ca.v5i2.4722

Nakada LYK, Urban RC (2020) COVID-19 pandemic: impacts on the air quality during the partial lockdown in São Paulo state Brazil. Sci Total Environ 730:139087. https://doi.org/10.1016/j.scitotenv.2020.139087

Negret PJ, Marco MD, Sonter LJ, Rhodes J, Possingham HP, Maron M (2020) Effects of spatial autocorrelation and sampling design on estimates of protected area effectiveness. Conserv Biol 34(6):1452–1462. https://doi.org/10.1111/cobi.13522

Nielsen O, Plejdrup MS, Dore C, et al (2019) EMEP/EEA air pollutant emission inventory guidebook 2019. http://www.envihaifa.org.il/prdFiles/1.A.4%20Small%20combustion%202019.pdf. Accessed 25December 2021

Okwir S, Ulfvengren P, Angelis J, Ruiz F, Guerrero YMN (2017) Managing turnaround performance through collaborative decision making. J Air Transp Manag 58:183–196. https://doi.org/10.1016/j.jairtraman.2016.10.008

Ping JL, Green CJ, Zartman RE, Bronson KF (2004) Exploring spatial dependence of cotton yield using global and local autocorrelation statistics. Field Crop Res 89(2–3):219–236. https://doi.org/10.1016/j.fcr.2004.02.009

Shi K, Weng J (2021) Impacts of the COVID-19 epidemic on merchant ship activity and pollution emissions in Shanghai port waters. Science of The Total Environment. https://doi.org/10.1016/j.scitotenv.2021.148198

Shi H, Zheng Y, Zhang X, Sun H (2021, October) Evaluation of residual airspace resources based on civil aviation operation big data. 2021 IEEE 3rd International Conference on Civil Aviation Safety and Information Technology (ICCASIT) 194–198. https://doi.org/10.1109/ICCASIT53235.2021.9633413.

Shirmohammadi F, Sowlat MH, Hasheminassab S et al (2017) Emission rates of particle number, mass and black carbon by the Los Angeles International Airport (LAX) and its impact on air quality in Los Angeles. Atmos Environ 151:82–93. https://doi.org/10.1016/j.atmosenv.2016.12.005

Simini F, González MC, Maritan A, Barabási AL (2012) A universal model for mobility and migration patterns. Nature 484(7392):96–100. https://doi.org/10.1038/nature10856

Song SK, Shon ZH (2012) Emissions of greenhouse gases and air pollutants from commercial aircraft at international airports in Korea. Atmos Environ 61:148–158. https://doi.org/10.1016/j.atmosenv.2012.07.035

Song Y, Huang B, He Q, Chen B, Wei J, Mahmood R (2019) Dynamic assessment of PM2. 5 exposure and health risk using remote sensing and geo-spatial big data. Environ Pollut 253:288–296. https://doi.org/10.1016/j.envpol.2019.06.057

Sun X, Wandelt S, Zhang A (2020) How did COVID-19 impact air transportation? A first peek through the lens of complex networks. J Air Transp Manag 89:101928. https://doi.org/10.1016/j.jairtraman.2020.101928

Sun X, Wandelt S, Zheng C, Zhang A (2021) COVID-19 pandemic and air transportation: successfully navigating the paper hurricane. J Air Transp Manag 94:102062. https://doi.org/10.1016/j.jairtraman.2021.102062

Tobler WR (1979) Smooth pycnophylactic interpolation for geographical regions. J Am Stat Assoc 74(367):519–530. https://doi.org/10.1080/01621459.1979.10481647

Tokuslu A (2020) Estimation of aircraft emissions at Georgian International Airport. Energy. https://doi.org/10.1016/j.energy.2020.118219

Tokuslu A (2021) Calculation of aircraft emissions during landing and take-off (LTO) cycles at Batumi International Airport. Georgia. Intl J Environ Geoinformatics 8(2):186–192. https://doi.org/10.30897/ijegeo.836780

Vink N (2021) The effect to human performance and wellbeing of air traffic management operational staff through the COVID-19 pandemic. In 91st International Symposium on Aviation Psychology (370)

Wang K, Fu X, Czerny AI, Hua G, Lei Z (2020) Modeling the potential for aviation liberalization in Central Asia–market analysis and implications for the belt and road initiative. Transp Res Part a: Policy Pract 134:184–210. https://doi.org/10.1016/j.tra.2020.02.004

Wu CL, Wang HW, Cai WJ et al (2021) Impact of the COVID-19 lockdown on roadside traffic-related air pollution in Shanghai. Building and environment, China. https://doi.org/10.1016/j.buildenv.2021.107718

Wu D, Wang X, Wu S (2022) Construction of stock portfolios based on k-means clustering of continuous trend features. Knowl-Based Syst 252:109358. https://doi.org/10.1016/j.knosys.2022.109358

Xiang J, Austin E, Gould T, et al (2020) Impacts of the COVID-19 responses on traffic-related air pollution in a Northwestern US city. Sci Total Environ. https://doi.org/10.1016/j.scitotenv.2020.141325

Xue D, Hsu LT, Wu CL, Lee CH, Ng KK (2021a) Cooperative surveillance systems and digital-technology enabler for a real-time standard terminal arrival schedule displacement. Adv Eng Inform 50:101402. https://doi.org/10.1016/j.aei.2021.101402

Xue D, Liu Z, Wang B, Yang J (2021b) Impacts of COVID-19 on aircraft usage and fuel consumption: a case study on four Chinese international airports. J Air Transp Manag 95:102106. https://doi.org/10.1016/j.jairtraman.2021.102106

Xue D, Yang J, Liu Z (2022) Potential impact of GNSS positioning errors on the satellite-navigation-based air traffic management. Space Weather, 20(7). https://doi.org/10.1029/2022SW003144

Yılmaz i (2017) Emissions from passenger aircraft at Kayseri Airport, Turkey. J Air Transp Manag 58:176–182. https://doi.org/10.1016/j.jairtraman.2016.11.001

Yu JI, Jia Q, Gao C, Hu HQ (2021) Air pollutant emissions from aircraft landing and take-off cycles at Chinese airports. Aeronaut J 125(1285):578–592. https://doi.org/10.1017/aer.2020.126

Zhang T, Ding M, Zuo H (2018) Improved approach for time-based taxi trajectory planning towards conflict-free, efficient and fluent airport ground movement. IET Intel Transport Syst 12(10):1360–1368. https://doi.org/10.1049/iet-its.2018.5193